Matrix-valued Boltzmann equation for the Hubbard chain

Martin L. R. Fürst[*]
Zentrum Mathematik, Boltzmannstraße 3, Technische Universität München and Excellence Cluster Universe, Boltzmannstraße 2, 85748 Garching bei München, Germany

Christian B. Mendl[†]
Zentrum Mathematik, Boltzmannstraße 3, Technische Universität München, 85748 Garching bei München, Germany

Herbert Spohn[‡]
Physik Department, James-Franck-Straße 1 and Zentrum Mathematik, Boltzmannstraße 3, Technische Universität München, 85748 Garching bei München, Germany

(Received 14 August 2012; published 18 September 2012)

We study, both analytically and numerically, the Boltzmann transport equation for the Hubbard chain with nearest-neighbor hopping and spatially homogeneous initial condition. The time-dependent Wigner function is matrix-valued because of spin. The H theorem holds. The nearest-neighbor chain is integrable, which, on the kinetic level, is reflected by infinitely many additional conservation laws and linked to the fact that there are also nonthermal stationary states. We characterize all stationary solutions. Numerically, we observe an exponentially fast convergence to stationarity and investigate the convergence rate in dependence on the initial conditions.

DOI: 10.1103/PhysRevE.86.031122 PACS number(s): 05.30.Fk, 67.10.Fj

I. INTRODUCTION

The Hubbard model is a simplified description of interacting electrons moving in a periodic background potential; see [1–3] for introductory literature. We are interested in the dynamics of the Hubbard model in the regime of small interactions, which is conveniently described by kinetic theory, following the pioneering work of Peierls [4], Nordheim [5], and Uehling and Uhlenbeck [6]. From the point of view of kinetic theory the Hubbard model has unusual features. The noninteracting model has a doubly degenerate band, which–because of spin–makes the Wigner function 2×2 matrix valued. In addition the Hamiltonian is invariant under global SU(2) spin rotations. On the kinetic level this property is reflected by an exceptionally large set of conserved quantities. We refer to [7] for a recent experimental realization through ultracold atoms in an optical lattice under conditions where also kinetic theory is applied.

As one would expect, even the matrix-valued Boltzmann equation satisfies the H theorem. The goal of our note is to achieve–beyond mere entropy increase–a quantitative and more detailed understanding of the approach to stationarity. The Boltzmann equation consists of the sum of an effective Hamiltonian plus a dissipative collision term, both with cubic nonlinearity. At such generality, numerical simulation is not an easy task. Therefore we concentrate on the Hubbard chain with nearest-neighbor hopping and on-site interaction. In addition we assume spatial homogeneity. Our simulations use 64 grid points in momentum space, which still allows for easy exploration. At this stage the reader might wonder why on the kinetic level in one dimension there are any collisions at all. This will be explained in due course, as well as the difference between the nearest-neighbor integrable model and the nonintegrable next-nearest-neighbor case.

Let us start with the underlying Hamiltonian and the resulting kinetic equation. The electrons are described by a spin-$\frac{1}{2}$ Fermi field on $\mathbb{Z}$ with creation and annihilation operators satisfying the anticommutation relations

$$\{a_\sigma^*(x), a_\tau(y)\} = \delta_{xy}\delta_{\sigma\tau}, \tag{1}$$

$$\{a_\sigma(x), a_\tau(y)\} = 0, \tag{2}$$

$$\{a_\sigma^*(x), a_\tau^*(y)\} = 0, \tag{3}$$

for $x, y \in \mathbb{Z}$, $\sigma, \tau \in \{\uparrow, \downarrow\}$, and $\{A, B\} = AB + BA$. The Hamiltonian reads

$$H = \sum_{x,y\in\mathbb{Z}} \alpha(x-y)\, a^*(x)\cdot a(y) + \frac{\lambda}{2}\sum_{x\in\mathbb{Z}} (a^*(x)\cdot a(x))^2. \tag{4}$$

Here $a^*(x)\cdot a(x) = a_\uparrow^*(x)\, a_\uparrow(x) + a_\downarrow^*(x)\, a_\downarrow(x)$. α is the hopping amplitude, with the properties $\alpha(x) = \alpha(x)^*$, $\alpha(x) = \alpha(-x)$, and λ is the strength of the on-site interaction. Our notation emphasizes the invariance under global spin rotations.

For the Fourier transformation we use the convention

$$\hat{f}(k) = \sum_{x\in\mathbb{Z}} f(x)\, \mathrm{e}^{-2\pi i\, k\, x}. \tag{5}$$

Then the first Brillouin zone is the interval $\mathbb{T} = [-\frac{1}{2}, \frac{1}{2}]$ with periodic boundary conditions. The dispersion relation $\omega(k) = \hat{\alpha}(k)$ and, up to a constant, in Fourier space H can be written as

$$H = \sum_{\sigma\in\{\uparrow,\downarrow\}} \int_{\mathbb{T}} dk\, \omega(k) \hat{a}_\sigma^*(k)\hat{a}_\sigma(k) + \frac{\lambda}{2}\int_{\mathbb{T}^4} d^4\boldsymbol{k}\, \delta(\underline{k})\, \hat{a}_\uparrow^*(k_1)\hat{a}_\uparrow^*(k_2)\hat{a}_\downarrow(k_3)\hat{a}_\downarrow(k_4), \tag{6}$$

with $\underline{k} = k_1 + k_2 - k_3 - k_4 \mod 1$ and $d^4\boldsymbol{k} = dk_1\, dk_2\, dk_3\, dk_4$.

[*]mfuerst@ma.tum.de
[†]mendl@ma.tum.de
[‡]spohn@ma.tum.de

To arrive at the kinetic equation, we assume that the initial state of the chain is quasifree, gauge invariant, and invariant under spatial translations. It is thus completely characterized by the two-point function

$$\langle \hat{a}^*_\sigma(k)\hat{a}_\tau(k')\rangle = \delta(k-k')W_{\sigma\tau}(k). \tag{7}$$

It will be convenient to think of $W(k)$ as a 2×2 matrix for each $k\in\mathbb{T}$. Then, in general, $W(k_1)W(k_2)\neq W(k_2)W(k_1)$ and every argument of standard kinetic theory has to be reworked. By the Fermi property we have $0\leqslant W(k)\leqslant 1$ as a matrix for each k. In particular, W can be written as

$$W(k)=\sum_{\sigma\in\{\uparrow,\downarrow\}}\varepsilon_\sigma(k)|k,\sigma\rangle\langle k,\sigma|, \tag{8}$$

where $|k,\sigma\rangle$ for $\sigma\in\{\uparrow,\downarrow\}$ is a k-dependent basis in spin space $\mathbb{C}^2$ and ε_σ are the eigenvalues with $0\leqslant\varepsilon_\sigma\leqslant 1$.

At some later time t the state is still gauge and translation invariant, hence necessarily

$$\langle a^*_\sigma(k,t)a_\tau(k',t)\rangle = \delta(k-k')W_{\sigma\tau}(k,t). \tag{9}$$

In general $W(t)$ is a complicated object, but for small coupling λ the quasifree property persists over a time scale of order λ^{-2}, a structure which allows one to obtain the kinetic equation by second order time-dependent perturbation theory. More details can be found, e.g., in [8–10]. Here we only write down the resulting Boltzmann equation:

$$\frac{\partial}{\partial t}W(k,t)=\mathcal{C}_{\rm c}[W](k,t)+\mathcal{C}_{\rm d}[W](k,t)=\mathcal{C}[W](k,t), \tag{10}$$

which has the structure of an evolution equation and has to be supplemented with the initial data $W(k,0)=W(k)$.

The first term is of the Vlasov type:

$$\mathcal{C}_{\rm c}[W](k,t)=-i\,[H_{\rm eff}(k,t),W(k,t)], \tag{11}$$

where the effective Hamiltonian $H_{\rm eff}(k,t)$ is a 2×2 matrix which itself depends on W. More explicitly,

$$\begin{aligned}H_{\rm eff,1}=&\int_{\mathbb{T}^3}dk_2dk_3dk_4\,\delta(\underline{k})\,\mathcal{P}\left(\frac{1}{\underline{\omega}}\right)\\&\times\big(W_3W_4-W_2W_3-W_3W_2\\&\qquad-\mathrm{tr}[W_4]W_3+\mathrm{tr}[W_2]W_3+W_2\big).\end{aligned} \tag{12}$$

Here and later on we use the shorthand $\tilde{W}=1-W$, $W_1=W(k_1,t)$, $H_{\rm eff,1}=H_{\rm eff}(k_1,t)$, $\underline{\omega}=\omega(k_1)+\omega(k_2)-\omega(k_3)-\omega(k_4)$. Since W is 2×2 matrix valued, $\mathrm{tr}[\,\cdot\,]$ is the trace in spin space. Finally $\mathcal{P}$ denotes the principal part. Since the k_3, k_4 integration can be interchanged, $H_{\rm eff}=H^*_{\rm eff}$, as it should be.

There are many different ways to write the collision term $\mathcal{C}_{\rm d}$. We choose a version which separates the various contributions into gain and loss terms. Then

$$\mathcal{C}_{\rm d}[W]_1=\pi\int_{\mathbb{T}^3}dk_2dk_3dk_4\delta(\underline{k})\delta(\underline{\omega})\big(\mathcal{A}[W]_{1234}+\mathcal{A}[W]^*_{1234}\big), \tag{13}$$

where the index 1234 means that the matrix $\mathcal{A}[W]$ depends on k_1, k_2, k_3, and k_4. Explicitly,

$$\begin{aligned}\mathcal{A}[W]_{1234}=&-W_4\tilde{W}_3W_2+W_4\,\mathrm{tr}[\tilde{W}_3W_2]\\&-\big\{\tilde{W}_4W_2-\tilde{W}_4W_3-\tilde{W}_3W_2+\tilde{W}_4\,\mathrm{tr}[W_3]\\&\qquad-\tilde{W}_4\,\mathrm{tr}[W_2]+\mathrm{tr}[W_2\tilde{W}_3]\big\}W_1,\end{aligned} \tag{14}$$

with the first two summands being the gain term and $\{...\}W_1$ being the loss term. The gain term is always positive definite, as implied by the inequality

$$A\,\mathrm{tr}[BC]+C\,\mathrm{tr}[BA]-ABC-CBA\geqslant 0, \tag{15}$$

valid for arbitrary positive definite matrices A,B,C. Thus if an eigenvalue of $W(k,t)$ happens to vanish, the gain term pushes it back to values >0. A similar argument can be made for $\tilde{W}(k,t)$, implying the propagation of the Fermi property [10], to say the following: if at $t=0$ one has $0\leqslant W(k)\leqslant 1$, then the solution to Eq. (10) also satisfies $0\leqslant W(k,t)\leqslant 1$.

In our contribution, we report on a numerical solution of the kinetic equation (10), emphasizing the approach to stationarity. To provide an outline, in Sec. II we establish a few general properties of Eqs. (10), (12), (13). They hold for arbitrary ω and also for the obvious extension of Eq. (10) to d dimensions. In particular, we show that the entropy production $\sigma[W]=\frac{d}{dt}S[W]$ has the property $\sigma\geqslant 0$. The thermal state $W_{\rm FD}$ (the Fermi-Dirac distribution) satisfies $\mathcal{C}[W_{\rm FD}]=0$ and hence also $\sigma[W_{\rm FD}]=0$. But to list all stationary solutions of Eq. (10) is not an easy task in general.

In Sec. III we restrict ourselves to the Hubbard chain with nearest-neighbor hopping, i.e.,

$$\omega(k)=1-\cos(2\pi k). \tag{16}$$

The first task is to discuss the kinematically allowed collisions, in other words the solutions of $\underline{\omega}=0$ together with $\underline{k}=0$ mod 1. The nearest-neighbor model has a special symmetry through which a large set of further stationary states, beyond the thermal ones, can be found. On the kinetic level, this reflects the integrability of the underlying quantum Hamiltonian. In Sec. IV our numerical procedure is outlined and in Sec. V it is used to study the dynamics for representative initial Wigner functions.

II. GENERAL PROPERTIES OF THE HUBBARD KINETIC EQUATION

To emphasize generality, for this section only, we consider $\mathbb{Z}^d$ as an underlying lattice. Hence $k_j\in\mathbb{T}^d$ with periodic boundary conditions. The SU(2) invariance of H is reflected by

$$\mathcal{C}[U^*WU]=U^*\mathcal{C}[W]U, \tag{17}$$

for all $U\in\mathrm{SU}(2)$. Hence if $W(k,t)$ is a solution to Eq. (10), so is $U^*\,W(k,t)\,U$. Also hermiticity is propagated in time, i.e., if $W(0)=W(0)^*$, then also $W(t)=W(t)^*$, which follows from

$$\mathcal{C}[W]^*=\mathcal{C}[W^*]. \tag{18}$$

Furthermore the Fermi property, $0\leqslant W(t)\leqslant 1$, is propagated in time; see [10] for details.

There are two conservation laws: spin,

$$\frac{d}{dt}\int_{\mathbb{T}^d}dk\;W(k,t)=0, \tag{19}$$

and energy,

$$\frac{d}{dt}\int_{\mathbb{T}^d}dk\;\omega(k)\,\mathrm{tr}[W(k,t)]=0. \tag{20}$$

The proof uses the symmetrization of the integrand. One can interchange the variables $k_1 \leftrightarrow k_2$, $k_3 \leftrightarrow k_4$ and also the pairs $\{k_1,k_2\} \leftrightarrow \{k_3,k_4\}$. For the energy, one then picks up the integrand $\underline{\omega}$ and hence the factor $\underline{\omega}\,\delta(\underline{\omega}) = 0$.

The next general property is the H theorem. Since $|\lambda| \ll 1$, locally the state is a free fermion. On the kinetic level, the entropy of the state W is then defined as

$$S[W] = -\int_{\mathbb{T}^d} dk_1(\mathrm{tr}[W_1 \log W_1] + \mathrm{tr}[\tilde{W}_1 \log \tilde{W}_1]). \tag{21}$$

Hence the entropy production is given by

$$\sigma[W] = \frac{d}{dt}S[W] = -\int_{\mathbb{T}^d} dk_1\,\mathrm{tr}[(\log W_1 - \log \tilde{W}_1)\,\mathcal{C}[W]_1]. \tag{22}$$

The H theorem asserts that

$$\sigma[W] \geqslant 0 \quad \text{for all } W \text{ with } 0 \leqslant W \leqslant 1. \tag{23}$$

To establish Eq. (23), for each k we write

$$W(k) = \sum_{\sigma\in\{\uparrow,\downarrow\}} \varepsilon_\sigma(k) P_\sigma(k), \tag{24}$$

with eigenvalues $0 \leqslant \varepsilon_\sigma(k) \leqslant 1$ and orthogonal eigenprojections $P_\sigma(k) = |k,\sigma\rangle\langle k,\sigma|$ with $\langle k,\sigma|k,\sigma'\rangle = \delta_{\sigma\sigma'}$. As before, we use a shorthand as $P_j = P_{\sigma_j}(k_j)$, $\varepsilon_j = \varepsilon_{\sigma_j}(k_j)$ and $\sum_{\boldsymbol{\sigma}} = \sum_{\sigma_1,\sigma_2,\sigma_3,\sigma_4}$. Inserting Eq. (24) into Eq. (22), one obtains

$$\begin{aligned}\sigma[W] &= \pi \int_{(\mathbb{T}^d)^4} d^4\boldsymbol{k}\,\delta(\underline{k})\delta(\underline{\omega}) \sum_{\boldsymbol{\sigma}} (\log\varepsilon_1 - \log\tilde{\varepsilon}_1) \\ &\quad \times (\tilde{\varepsilon}_1\tilde{\varepsilon}_2\varepsilon_3\varepsilon_4 - \varepsilon_1\varepsilon_2\tilde{\varepsilon}_3\tilde{\varepsilon}_4)(\mathrm{tr}[P_1P_3]\mathrm{tr}[P_2P_4] \\ &\quad + \mathrm{tr}[P_1P_3]\mathrm{tr}[P_2P_4] - \mathrm{tr}[P_1P_3P_2P_4] - \mathrm{tr}[P_4P_2P_3P_1]) \\ &= \pi \int_{(\mathbb{T}^d)^4} d^4\boldsymbol{k}\,\delta(\underline{k})\delta(\underline{\omega}) \sum_{\boldsymbol{\sigma}} (\tilde{\varepsilon}_1\tilde{\varepsilon}_2\varepsilon_3\varepsilon_4 - \varepsilon_1\varepsilon_2\tilde{\varepsilon}_3\tilde{\varepsilon}_4) \\ &\quad \times \log(\tilde{\varepsilon_1}/\varepsilon_1)\,|\langle k_1,\sigma_1|k_3,\sigma_3\rangle\langle k_2,\sigma_2|k_4,\sigma_4\rangle \\ &\quad - \langle k_1,\sigma_1|k_4,\sigma_4\rangle\langle k_2,\sigma_2|k_3,\sigma_3\rangle|^2. \end{aligned} \tag{25}$$

We interchange $1 \leftrightarrow 2$, $3 \leftrightarrow 4$ and $(1,2) \leftrightarrow (3,4)$. Then

$$\begin{aligned}\sigma[W] &= \frac{\pi}{4} \int_{(\mathbb{T}^d)^4} d^4\boldsymbol{k}\,\delta(\underline{k})\delta(\underline{\omega}) \sum_{\boldsymbol{\sigma}} (\tilde{\varepsilon}_1\tilde{\varepsilon}_2\varepsilon_3\varepsilon_4 - \varepsilon_1\varepsilon_2\tilde{\varepsilon}_3\tilde{\varepsilon}_4) \\ &\quad \times \log\left(\frac{\tilde{\varepsilon}_1\tilde{\varepsilon}_2\varepsilon_3\varepsilon_4}{\varepsilon_1\varepsilon_2\tilde{\varepsilon}_3\tilde{\varepsilon}_4}\right) |\langle k_1,\sigma_1|k_3,\sigma_3\rangle\langle k_2,\sigma_2|k_4,\sigma_4\rangle \\ &\quad - \langle k_1,\sigma_1|k_4,\sigma_4\rangle\langle k_2,\sigma_2|k_3,\sigma_3\rangle|^2 \geqslant 0, \end{aligned} \tag{26}$$

since $(x-y)\log(x/y) \geqslant 0$.

Stationary states are defined by

$$\mathcal{C}[W] = 0, \tag{27}$$

which obviously implies $\sigma[W] = 0$. Physically one would expect thermal equilibrium to be included in the stationary states. On the kinetic level thermal equilibrium is defined by the Fermi-Dirac state:

$$W_{\mathrm{FD}}(k) = \sum_{\sigma\in\{\uparrow,\downarrow\}} \left(\mathrm{e}^{\beta(\omega(k)-\mu_\sigma)} + 1\right)^{-1} |\sigma\rangle\langle\sigma|, \tag{28}$$

which is characterized by the inverse temperature β, the two chemical potentials $\mu_\uparrow$, $\mu_\downarrow$ for the spin occupations, and some k-independent spin basis $|\sigma\rangle$, β, $\mu_\uparrow$, $\mu_\downarrow \in \mathbb{R}$. Indeed, it is easily checked that $\mathcal{C}[W_{\mathrm{FD}}] = 0$.

With this background information, one develops the following rough picture on the approach to stationarity. The initial state determines a special, k-independent basis $|\sigma\rangle$ through

$$\int_{\mathbb{T}^d} dk\,W(k) = \sum_{\sigma\in\{\uparrow,\downarrow\}} \varepsilon_\sigma\,|\sigma\rangle\langle\sigma|. \tag{29}$$

By Eq. (19) this basis is preserved in time. Thus it is natural to expand $W(k,t)$ in this special basis. Approach to the thermal state would mean

$$\lim_{t\to\infty} \langle\sigma|W(k,t)|\sigma'\rangle = 0 \quad \text{for} \quad \sigma \neq \sigma' \tag{30}$$

and

$$\lim_{t\to\infty} \langle\sigma|W(k,t)|\sigma\rangle = \left(\mathrm{e}^{\beta(\omega(k)-\mu_\sigma)} + 1\right)^{-1} \quad \text{for} \quad \sigma \in \{\uparrow,\downarrow\}. \tag{31}$$

Since, by Eq. (19), the integral over the eigenvalue is conserved, one concludes that

$$\varepsilon_\sigma = \int_{\mathbb{T}^d} dk \left(\mathrm{e}^{\beta(\omega(k)-\mu_\sigma)} + 1\right)^{-1}, \quad \sigma \in \{\uparrow,\downarrow\}. \tag{32}$$

Correspondingly, by Eq. (20), for the average energy,

$$\begin{aligned}\mathsf{e} &= \int_{\mathbb{T}^d} dk\,\omega(k)\,\mathrm{tr}[W(k)] \\ &= \int_{\mathbb{T}^d} dk \sum_{\sigma\in\{\uparrow,\downarrow\}} \omega(k)\left(\mathrm{e}^{\beta(\omega(k)-\mu_\sigma)} + 1\right)^{-1}. \end{aligned} \tag{33}$$

Both equations determine the parameters β, $\mu_\uparrow$, $\mu_\downarrow$ from the initial W. One has $0 \leqslant \varepsilon_\uparrow,\varepsilon_\downarrow \leqslant 1$ and $\min_k \omega(k) \leqslant \mathsf{e}/2 \leqslant \max_k \omega(k)$. Then the map $(\mathsf{e},\varepsilon_\uparrow,\varepsilon_\downarrow)$ to $(\beta,\mu_\uparrow,\mu_\downarrow)$ is one to one.

Implicitly our argument assumes that the set of stationary states equals the set of thermal states. But this might fail if there are not enough collisions, which could very well be the case in low dimensions. The issue of characterizing all stationary states has been accomplished only partially; see [11] for results towards this goal. On the other hand we still succeed in listing all stationary states and their domain of attraction. As will be discussed in the following section, for the Hubbard chain with nearest-neighbor hopping the stationary states are not exhausted by the thermal ones.

III. NEAREST-NEIGHBOR HUBBARD CHAIN

A. Collisions

We return to the Hubbard chain with nearest-neighbor hopping [Eq. (16)]. Figure 1 visualizes $\omega(k)$ for $k \in [-\frac{1}{2},\frac{1}{2}]$. The first task is to investigate the kinematically allowed collisions defined by $\delta(\underline{k})\delta(\underline{\omega})$. The momentum conservation $\underline{k} = 0 \mod 1$ allows us to eliminate one k variable, say $k_2 = k_3 + k_4 - k_1 \mod 1$. Inserted into energy conservation $\underline{\omega} = 0$ and using some trigonometric identities, one arrives at

$$\underline{\omega} = 4\sin(\pi(k_1-k_3))\sin(\pi(k_1-k_4))\cos(\pi(k_3+k_4)). \tag{34}$$

Figure 2 visualizes $\underline{\omega}$ for fixed $k_1 = \frac{23}{64}$. From Eq. (34), we conclude that the collision manifold has a solution path $k_3 + k_4 = \frac{1}{2}$ (and thus also $k_1 + k_2 = \frac{1}{2}$) denoted γ_{diag} in Fig. 2,

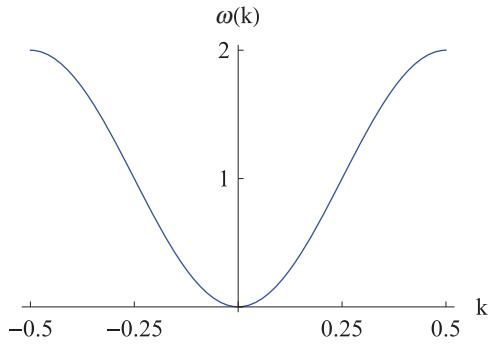

FIG. 1. (Color online) The dispersion relation $\omega(k)$ of Eq. (16).

besides the "trivial" solutions $k_3 = k_1$ (denoted γ_1) and $k_4 = k_1$ (denoted γ_2).

In what follows, we investigate the integral (13) of the dissipative collision operator C_d along the paths γ_1, γ_2, and γ_{diag}. Using the invariance of the integral (13) under $k_3 \leftrightarrow k_4$, we may interchange $W_3 \leftrightarrow W_4$. Then the integrand in Eq. (13) can be decomposed as

$$\mathcal{A}[W]_{1234} + \mathcal{A}[W]^*_{1234} = \mathcal{A}_{\text{quad}}[W]_{1234} + \mathcal{A}_{\text{tr}}[W]_{1234}, \quad (35)$$

with

$$\mathcal{A}_{\text{quad}}[W]_{1234} = -\tilde{W}_1 W_3 \tilde{W}_2 W_4 - W_4 \tilde{W}_2 W_3 \tilde{W}_1 + W_1 \tilde{W}_3 W_2 \tilde{W}_4 + \tilde{W}_4 W_2 \tilde{W}_3 W_1, \quad (36)$$

$$\mathcal{A}_{\text{tr}}[W]_{1234} = (\tilde{W}_1 W_3 + W_3 \tilde{W}_1)\text{tr}[\tilde{W}_2 W_4] - (W_1 \tilde{W}_3 + \tilde{W}_3 W_1)\text{tr}[W_2 \tilde{W}_4]. \quad (37)$$

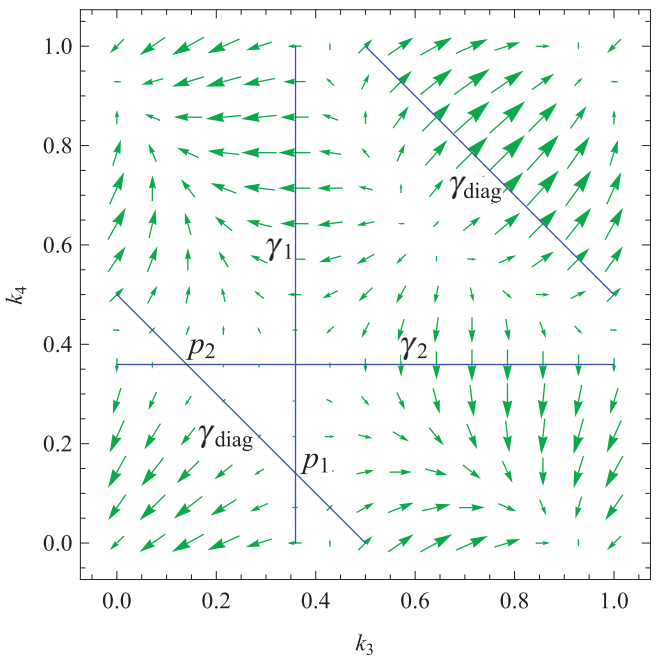

FIG. 2. (Color online) Contour (blue straight lines) and gradient (green vectors) of the energy conservation $\omega = 0$ for fixed $k_1 = \frac{23}{64}$ and after eliminating k_2. The diagonal blue line γ_{diag} is precisely the contour $k_3 + k_4 = \frac{1}{2}$. The vertical and horizontal blue lines, γ_1 and γ_2, are the contours $k_3 = k_1$ and $k_4 = k_1$, respectively. p_i marks the intersection of γ_i with γ_{diag} for $i = 1,2$.

Inspection of Eq. (36) immediately reveals that $\mathcal{A}_{\text{quad}}[W]_{1221} \equiv 0$ along γ_2 since $(k_1,k_2) = (k_4,k_3)$. Moreover, we also have $\mathcal{A}_{\text{quad}}[W]_{1212} \equiv 0$ along γ_1 with $(k_1,k_2) = (k_3,k_4)$, which can be checked by expanding Eq. (36). In other words, $\mathcal{A}_{\text{quad}}[W]_{1234}$ contributes only along γ_{diag}.

The situation is different for the term $\mathcal{A}_{\text{tr}}[W]_{1234}$: while $\mathcal{A}_{\text{tr}}[W]_{1212} \equiv 0$ along γ_1 by direct inspection of Eq. (37), it is (in general) nonzero along γ_2 and also along γ_{diag}. In summary, for evaluating the dissipative collision integral Eq. (13) we have to integrate $\mathcal{A}_{\text{tr}}[W]$ along γ_2 and both $\mathcal{A}_{\text{quad}}[W]$ and $\mathcal{A}_{\text{tr}}[W]$ along γ_{diag}.

As a side remark, the solution path γ_{diag} is special for the nearest-neighbor dispersion relation Eq. (16). If we add to Eq. (16) a small next-nearest-neighbor term, then γ_1 and γ_2 persist and γ_{diag} gets somewhat deformed. In addition, a new collision channel opens up, as illustrated in Fig. 3 for the dispersion relation

$$\omega_{\text{nnn}}(k) = \omega(k) - \tfrac{1}{2}\cos(4\pi k) = 1 - \cos(2\pi k) - \tfrac{1}{2}\cos(4\pi k). \quad (38)$$

B. Stationary solutions

The collision paths γ_1, γ_2, and γ_{diag} have special symmetries, from which one can guess the form of stationary solutions beyond the thermal one. They have the same structure as the Fermi-Dirac state, but with $\omega(k)$ replaced by a more general function f. One finds

$$W_{\text{st}}(k) = \sum_{\sigma\in\{\uparrow,\downarrow\}} \lambda_\sigma(k)\,|\sigma\rangle\langle\sigma|, \quad \lambda_\sigma(k) = \left(e^{f(k)-a_\sigma} + 1\right)^{-1}, \quad (39)$$

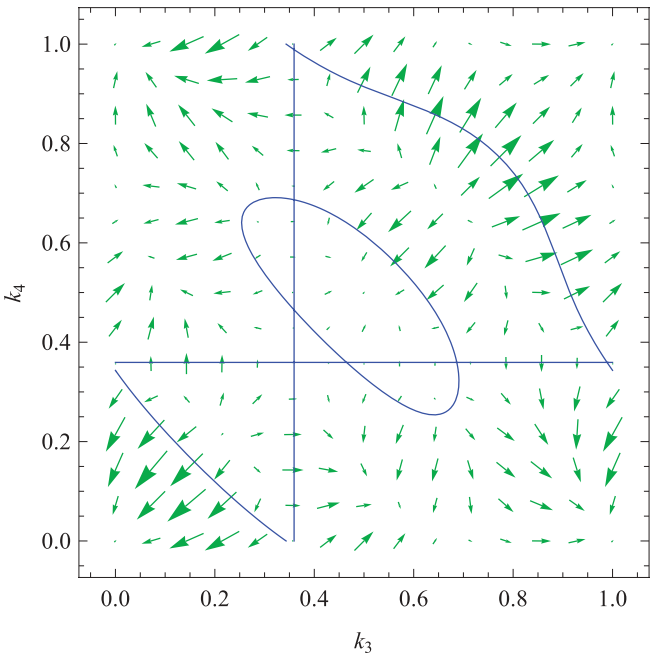

FIG. 3. (Color online) Contour (blue straight lines) and gradient (green vectors) of the energy conservation for a next-nearest-neighbor model with $\omega_{\text{nnn}}(k)$ of Eq. (38) and fixed $k_1 = \frac{23}{64}$.

where f is a real-valued, one-periodic function satisfying $f(k) = -f(\frac{1}{2} - k)$, $a_\sigma \in \mathbb{R}$, and $|\sigma\rangle$ is an orthogonal basis, independent of k.

As discussed in the Appendix, Eq. (39) characterizes the entire set of stationary solutions. The next step is to identify the domain of attraction for W_{st}, in other words to study the map from the initial W to W_{st}. Here we can follow the strategy described at the end of Sec. II.

We first note that there are many energy-like quantities which are conserved. Let $g : \mathbb{T} \to \mathbb{R}$ with $g(k) = -g(\frac{1}{2} - k)$. Then

$$\frac{d}{dt} \int_{\mathbb{T}} dk\, g(k)\, \mathrm{tr}[W(k)] = 0, \tag{40}$$

which generalizes the energy conservation Eq. (20). Equation (40) again follows by an appropriate interchange of the integration variables $k_1, \ldots, k_4$.

By substituting $g(k) = \delta(k - k') - \delta(k - \frac{1}{2} + k')$ for arbitrary $k' \in \mathbb{T}$, one concludes that

$$h(k) = \mathrm{tr}[W(k)] - \mathrm{tr}\big[W\big(\tfrac{1}{2} - k\big)\big] \tag{41}$$

is pointwise constant for each $k \in \mathbb{T}$. Assuming that the initial W converges to a stationary state of the form of Eq. (39), it must hold that

$$h(k) = \sum_{\sigma\in\{\uparrow,\downarrow\}} \Big(\big(\mathrm{e}^{f(k)-a_\sigma} + 1\big)^{-1} - \big(\mathrm{e}^{-f(k)-a_\sigma} + 1\big)^{-1}\Big). \tag{42}$$

Equivalently, as in Sec. II, the spin conservation law requires that the eigenvalues ε_σ in Eq. (29) are equal to

$$\varepsilon_\sigma = \int_{\mathbb{T}} dk\, \big(\mathrm{e}^{f(k)-a_\sigma} + 1\big)^{-1}. \tag{43}$$

We claim that Eqs. (42) and (43) uniquely determine f and a_σ, or more specifically, that the map between

$$\mathrm{tr}[W(k)] - \mathrm{tr}\big[W\big(\tfrac{1}{2} - k\big)\big], \quad |k| \leqslant \tfrac{1}{4}, \quad 0 \leqslant \varepsilon_\uparrow, \varepsilon_\downarrow \leqslant 1 \tag{44}$$

and

$$f(k) \text{ with } f(k) = -f\big(\tfrac{1}{2} - k\big), \quad |k| \leqslant \tfrac{1}{4}, \quad a_\uparrow, a_\downarrow \tag{45}$$

is one to one. In particular, to a given W one can associate a unique W_{st} of the form of Eq. (39).

Sketch of the proof. By a short calculation, Eq. (42) can be written as

$$h(k) = -\sinh(f(k)) \times \left(\frac{1}{\cosh a_\uparrow + \cosh f(k)} + \frac{1}{\cosh a_\downarrow + \cosh f(k)}\right), \tag{46}$$

and Eq. (43) can be written as

$$\varepsilon_\sigma = \int_{\mathrm{I}} dk \left(\frac{\sinh a_\sigma}{\cosh a_\sigma + \cosh f(k)} + 1\right), \tag{47}$$

with interval of integration $\mathrm{I} := [-\frac{1}{4}, \frac{1}{4}]$. We define a generalized "free energy" through

$$H(f, a_\uparrow, a_\downarrow) = \int_{\mathrm{I}} dk \sum_{\sigma\in\{\uparrow,\downarrow\}} \log\big(\cosh a_\sigma + \cosh f(k)\big). \tag{48}$$

The map $(f, a_\uparrow, a_\downarrow) \mapsto H$ is strictly convex. Furthermore,

$$\frac{\partial}{\partial a_\sigma} H = \int_{\mathrm{I}} dk \frac{\sinh a_\sigma}{\cosh a_\sigma + \cosh f(k)} = \varepsilon_\sigma - \frac{1}{2} \tag{49}$$

and

$$\frac{\delta H}{\delta f(k)} = \sum_{\sigma\in\{\uparrow,\downarrow\}} \frac{\sinh f(k)}{\cosh a_\sigma + \cosh f(k)} = -h(k). \tag{50}$$

Thus the map from above can be viewed as Legendre transform from the first set Eq. (44) to the second set of variables Eq. (45). Since H is convex, the map is one to one. ■

IV. NUMERICAL PROCEDURE

A. Mollifying the collision operators

Dissipative collision operator. We have to make sure that $\delta(\underline{\omega})\delta(\underline{k})$ is a well-defined prescription. For this purpose we eliminate k_2 and, using Eq. (34), obtain

$$\int_{\gamma_2} dk_4\, \delta(\underline{\omega}) = \big|\partial_{k_4}\underline{\omega}|_{k_4=k_1}\big|^{-1} = \big(2\pi\,|\sin(2\pi k_3) - \sin(2\pi k_1)|\big)^{-1}. \tag{51}$$

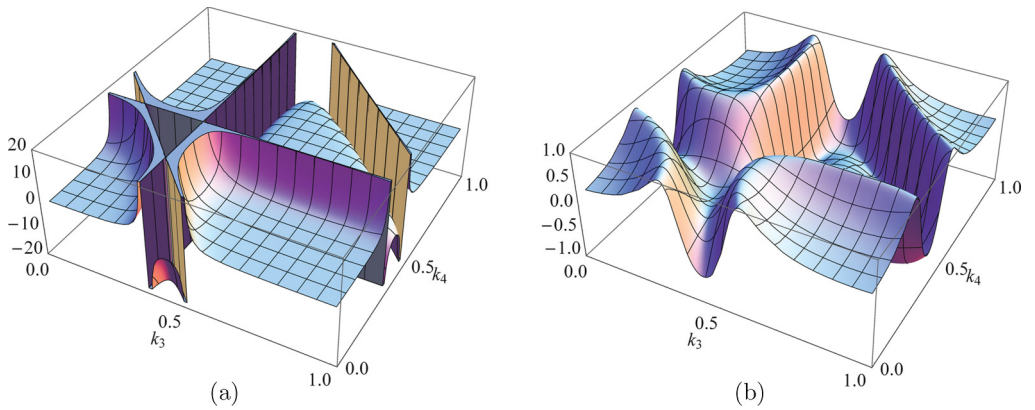

FIG. 4. (Color online) (a) The term $1/\underline{\omega}$ as a function of k_3 and k_4, for fixed $k_1 = 23/64$. (b) The "mollified" version $\underline{\omega}/(\underline{\omega}^2 + \epsilon^2)$ with $\epsilon = \frac{1}{2}$ free of singularities.

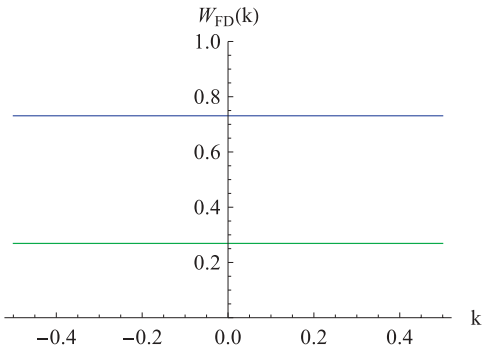

FIG. 5. (Color online) Diagonal matrix entries of a high-temperature equilibrium state W_{FD}. The state is (almost) independent of k.

Likewise along γ_{diag} it holds that

$$\int_{\gamma_{\mathrm{diag}}} dk_4\, \delta(\underline{\omega}) = \left|\partial_{k_4}\underline{\omega}|_{k_4=1/2-k_3}\right|^{-1} = \left(2\pi\,|\sin(2\pi k_3)-\sin(2\pi k_1)|\right)^{-1}. \quad (52)$$

Considering the subsequent integration over k_3 in Eq. (13), the critical point $k_3 = \frac{1}{2} - k_1$ (marked p_2 in Fig. 2) would lead to infinities in general. (Integrating along γ_{diag} across the point p_1 ($k_3 = k_1$) is possible since $\mathcal{A}[W]_{1234} + \mathcal{A}[W]^*_{1234}$ is zero at that point, as explained above.) As mollification we choose the substitution

$$\left(2\pi\,|\sin(2\pi k_3)-\sin(2\pi k_1)|\right)^{-1} \to \left(4\pi^2\big(\sin(2\pi k_3)-\sin(2\pi k_1)\big)^2+\epsilon^2\right)^{-1/2}, \quad (53)$$

with some finite $\epsilon > 0$. Concretely, we use $\epsilon = \frac{1}{2}$ for the simulations.

Conservative collision operator. The integral Eq. (12) for the conservative collision operator $\mathcal{C}_{\mathrm{c}}$ differs from dissipative integral Eq. (13), since there is only a single delta distribution $\delta(\underline{k})$. Thus, we can eliminate $k_2 = k_3 + k_4 - k_1$ as for the dissipative case, but still have to integrate over both k_3 and k_4.

The integral Eq. (12) is defined as Cauchy principal value with respect to $1/\underline{\omega}$. Figure 4(a) illustrates this term in dependence of k_3 and k_4 (compare also with Fig. 2). While the Cauchy principal value exists for continuous $W(k)$, the numeric calculation is rather demanding and we resort to a mollifying procedure as for the dissipative collision operator. Concretely, we substitute

$$\frac{1}{\underline{\omega}} \to \frac{\underline{\omega}}{\underline{\omega}^2+\epsilon^2} \quad (54)$$

with finite $\epsilon > 0$ (in our case $\epsilon = \frac{1}{2}$). Figure 4(b) shows the right-hand side, in direct comparison with the unmollified version. Note that $\mathcal{C}_{\mathrm{c}}$ could be defined via the integral Eq. (12) with the replacement Eq. (54), and then letting $\epsilon \to 0$.

B. Solving the Boltzmann equation

In order to solve the Boltzmann equation Eq. (10) numerically, we discretize the k variable by a uniform grid:

$$k_j = \frac{j}{n}, \quad j = 0,\ldots,n-1, \quad (55)$$

with $n = 64$ in our case. We have chosen the interval $[0,1]$ instead of (equivalently) $[-\frac{1}{2},\frac{1}{2}]$ simply for convenience. Note that due to periodicity, $W(1,t) = W(0,t)$, so the point $k = 1$ is not required. We use the trapezoidal rule to approximate the integrals (13) and (12) of the dissipative and conservative collision operators, respectively. Note that this approach is particularly suited for analytic period functions. Moreover, considering the two-dimensional integral of the conservative collision operator, we ensure that the variable $k_2 = k_3 + k_4 - k_1 \mod 1$ is a grid point whenever k_1, k_3 and k_4 are grid points, in distinction from other integration rules with nonuniform points.

We solve the Boltzmann differential equation (10) for the time variable by a *Strang splitting* (or *symmetric Trotter splitting*) technique: denoting the (fixed) time step by Δt, we combine an explicit midpoint rule step for the dissipative part with the time evolution operator for the conservative part:

$$X(k_j,t) = \mathrm{e}^{-i\,H_{\mathrm{eff}}(k_j,t)\,\Delta t/2}\, W(k_j,t)\, \mathrm{e}^{i\,H_{\mathrm{eff}}(k_j,t)\,\Delta t/2}, \quad j = 0,\ldots,n-1, \quad (56)$$

$$Y(k_j,t) = X(k_j,t) + \Delta t\, \mathcal{C}_{\mathrm{d}}\left[X(t) + \frac{\Delta t}{2}\mathcal{C}_{\mathrm{d}}[X(t)]\right](k_j), \quad j = 0,\ldots,n-1, \quad (57)$$

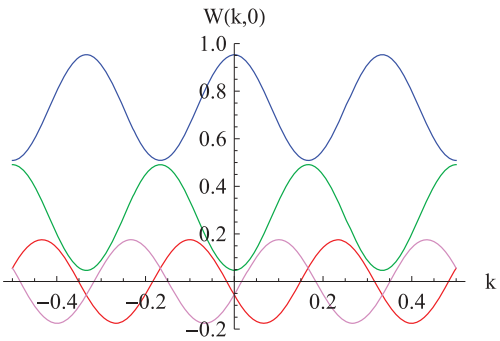

(a) matrix entries of initial $W(k,0)$

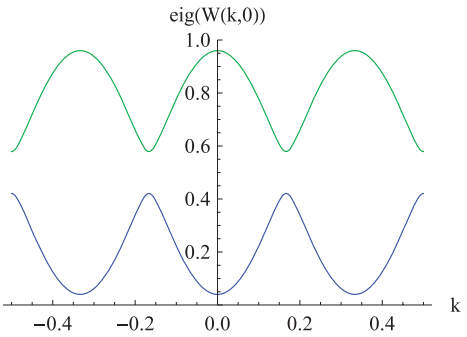

(b) eigenvalues of $W(k,0)$

FIG. 6. (Color online) (a) Initial state $W(k,0) = W_{\mathrm{FD}}(k) + V(k)$ with $V(k)$ defined in Eq. (59). The blue (upper) and green (middle) curves show the real diagonal entries, and the red (lower dark gray) and magenta (lower light gray) curves show the real and imaginary parts of the off-diagonal $|\uparrow\rangle\langle\downarrow|$ entry, respectively. (b) Corresponding eigenvalues of $W(k,0)$ in the interval $[0,1]$.

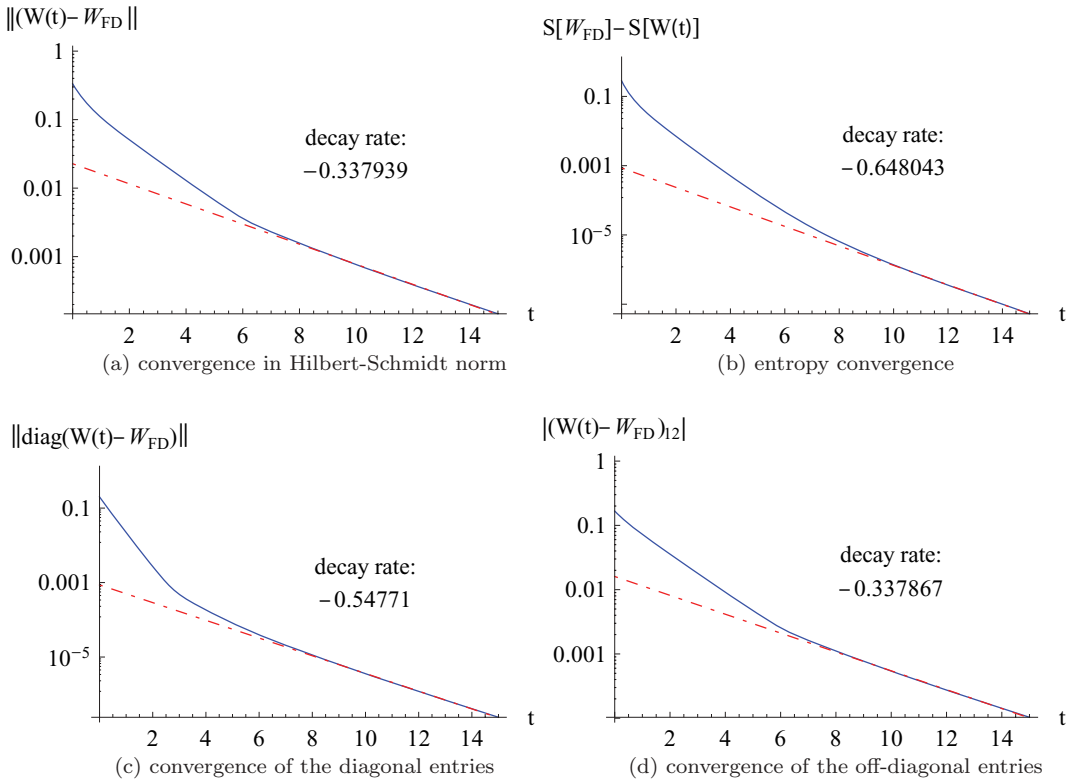

FIG. 7. (Color online) Convergence of the initial $W(0)$ (Fig. 6) to the high-temperature equilibrium state W_{FD} (Fig. 5) as a semilogarithmic plot (blue). The decay rate is the slope of the fitted red (dotted) line.

$$W(k_j,t+\Delta t) = \mathrm{e}^{-iH'_{\mathrm{eff}}(k_j,t)\,\Delta t/2}\, Y(k_j,t)\, \mathrm{e}^{iH'_{\mathrm{eff}}(k_j,t)\,\Delta t/2}, \quad j = 0,\ldots,n-1, \tag{58}$$

where H'_{eff} depends on $Y(t)$. The midpoint rule has order 2, while the time evolution operator $\mathrm{e}^{-iH\,\Delta t/2}(\cdot)\mathrm{e}^{iH\,\Delta t/2}$ has only order 1. Thus, the complete integration scheme has order 1. As advantage, the time evolution operator preserves matrix symmetry. For the simulations, we use $\Delta t = 1/16$, and the overall simulation time interval runs from $t = 0$ to varying upper limit $t = 15,\ldots,45$.

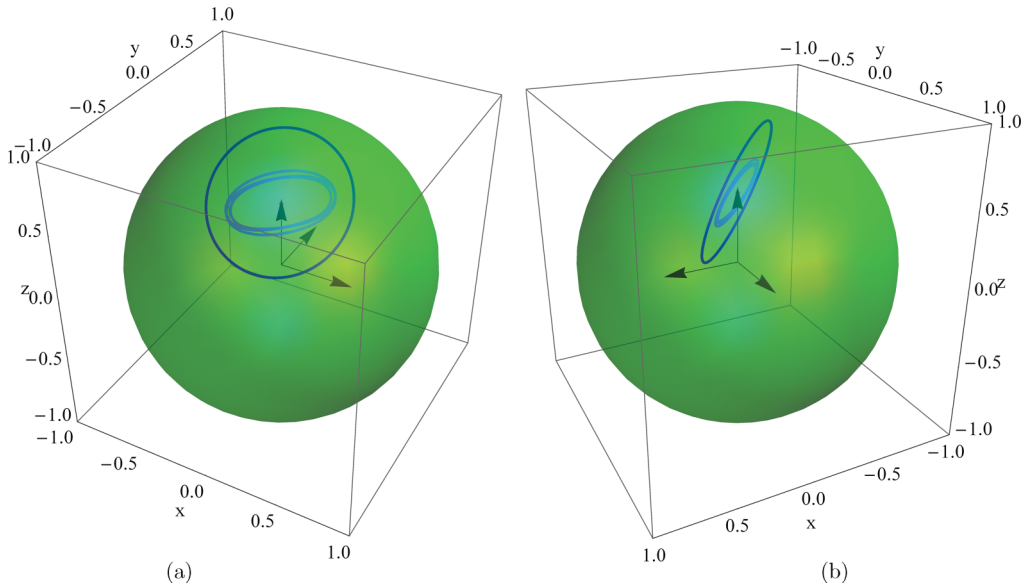

FIG. 8. (Color online) Bloch sphere representation (dark blue curve) of the initial $W(k,0)$ (Fig. 6), parametrized by k and viewed from two perspectives. The light blue curve shows the corresponding Bloch curve of $W(k,t)$ for $t = 1/2$. Finally, the curve for the high-temperature equilibrium state $W_{\mathrm{FD}}(k)$ is indiscernible from a single point at the tip of the z-axis arrow.

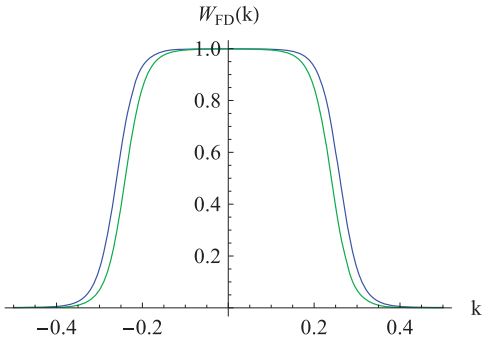

FIG. 9. (Color online) Diagonal matrix entries of a low-temperature equilibrium state W_{FD} ($\beta = 7$, $\mu_\uparrow = \frac{17}{16}$, $\mu_\downarrow = \frac{15}{16}$).

C. Cost analysis

Considering a single time step, the most expensive part is the evaluation of the conservative collision operator $\mathcal{C}_{\mathrm{c}}$ in Eqs. (56) and (58), i.e., the two-dimensional integral Eq. (12) after eliminating k_2. (The dissipative collision operator $\mathcal{C}_{\mathrm{d}}$ requires only a one-dimensional integration.) For the uniform discretization with n points in each direction, this scales like $O(n^2)$. One time step requires the evaluation of this integral for n different k_1 points, thus the overall cost is $O(n^3)$.

On a Intel Core i7-740QM Processor (6M cache, 1.73 GHz) without using parallelization, one time step takes approximately 90 s (Mathematica 8 implementation), so a complete simulation is approximately 6 h. Note that the performance could be easily increased by a C/C++ implementation and making use of parallelization.

V. SIMULATION RESULTS

1. High-temperature state

Figure 5 illustrates a high-temperature Fermi-Dirac equilibrium state W_{FD} Eq. (28) where $\beta = 10^{-4}$, $\mu_\uparrow = 10^4$ and $\mu_\downarrow = -10^4$. We have chosen the initial state (see Fig. 6) by $W(k,0) = W_{\mathrm{FD}}(k) + V(k)$ with $V(k)$ a rotation of the Pauli σ_z matrix and subtracting the constant matrix $\tau/18$:

$$V(k) = \frac{1}{4} \mathrm{e}^{-2\pi i\, \tau\, k}\, \sigma_z\, \mathrm{e}^{2\pi i\, \tau\, k} - \frac{\tau}{18}, \quad \tau = \sigma_x - \sigma_y + \frac{1}{2}\sigma_z. \tag{59}$$

$V(k)$ satisfies

$$\int_{\mathbb{T}} dk\, V(k) = 0 \quad \text{and} \quad \mathrm{tr}[V(k)] = 0, \tag{60}$$

for all $k \in \mathbb{T}$ such that $W(0)$ matches W_{FD} in terms of the spin and energy conservation laws Eqs. (19) and (20).

Figure 7 illustrates the convergence to the equilibrium state W_{FD}. Interestingly, we observe that the off-diagonal entries converge *slower* than the diagonal entries, but an analytic explanation of this effect is still lacking.

Figure 8 displays the Bloch vectors $\vec{r}(k,t) \in \mathbb{R}^3$ of $W(k,t)$ parametrized by k, i.e.,

$$W(k,t) = \tfrac{1}{2}\,(\mathbb{1} + \vec{r}(k,t)\cdot\vec{\sigma})\,, \quad \vec{\sigma} = (\sigma_x, \sigma_y, \sigma_z). \tag{61}$$

The dark blue curve shows the initial $\vec{r}(k,0)$ and the lighter blue curve shows $\vec{r}(k,\frac{1}{2})$. As time progresses, the initial curve straps to almost a single point, since $W_{\mathrm{FD}}(k)$ is almost independent of k.

2. Low-temperature state

Figure 9 illustrates a low-temperature Fermi-Dirac equilibrium state W_{FD} Eq. (28) with $\beta = 7$, $\mu_\uparrow = \frac{17}{16}$, and $\mu_\downarrow = \frac{15}{16}$.

In this case, for given $W_{\mathrm{FD}}(k)$ the variational freedom for the initial $W(k,0)$ with the same symmetries as $W_{\mathrm{FD}}(k)$ is strongly restricted. Similar to the high-temperature state, we define $W(k,0) = W_{\mathrm{FD}}(k) + V(k)$ (see Fig. 10) with

$$V(k) = \tfrac{1}{4}\big(\mathrm{e}^{-64\sin(\pi(k-3/4))^2} - \mathrm{e}^{-64\sin(\pi(k-1/4))^2}\big) \times \mathrm{e}^{-2\pi i\, \sigma_x\, k}\, \sigma_z\, \mathrm{e}^{2\pi i\, \sigma_x\, k}. \tag{62}$$

Again, $V(k)$ satisfies

$$\int_{\mathbb{T}} dk\, V(k) = 0 \quad \text{and} \quad \mathrm{tr}[V(k)] = 0, \tag{63}$$

for all $k \in \mathbb{T}$. We observe that the convergence to the equilibrium state (Fig. 11) is slower than for the high-temperature state in the previous paragraph. (Note that the simulation time interval is now [0,45] as compared to [0,15].)

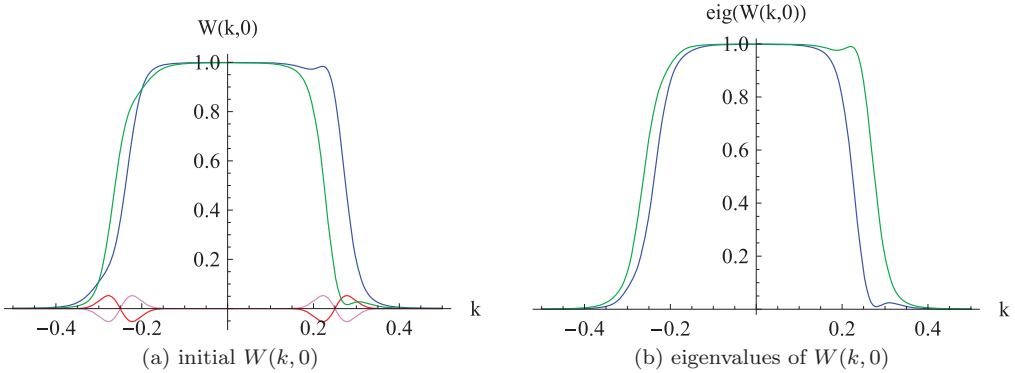

(a) initial $W(k,0)$ (b) eigenvalues of $W(k,0)$

FIG. 10. (Color online) (a) Initial state $W(k,0) = W_{\mathrm{FD}}(k) + V(k)$ with $V(k)$ defined in Eq. (62). The blue (upper right) and green (upper centered) curves show the real diagonal entries, and the red (lower dark gray) and magenta (lower light gray) curves show the purely imaginary off-diagonal entries. (b) Eigenvalues of $W(k,0)$ in the interval [0,1].

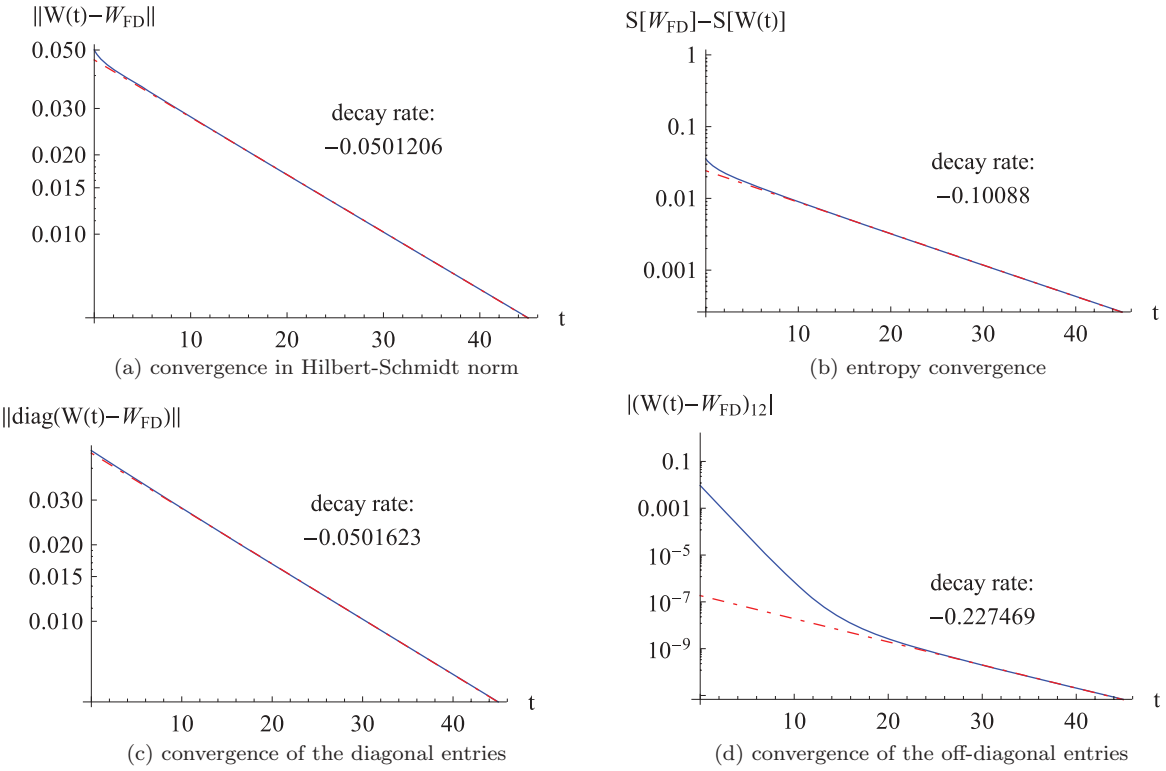

FIG. 11. (Color online) Convergence to the low-temperature equilibrium state W_{FD} (Fig. 9) as a semilogarithmic plot (blue). The decay rate is the slope of the fitted red (dotted) line. For this example, we observe that the off-diagonal entries converge much faster than the diagonal ones.

3. *Degenerate chemical potentials*

We consider a Fermi-Dirac equilibrium state with degenerate chemical potentials $\mu_\uparrow = \mu_\downarrow$, as illustrated in Fig. 12. As initial state $W(k,0)$, we set $W(k,0) = W_{\mathrm{FD}}(k) + V(k)$ (see Fig. 13) with $V(k)$ taken from Eq. (59). As illustrated in Fig. 14, there is no indication that the convergence changes due to the degeneracy. Two time snapshots of the eigenvalues of $W(k,t)$ are shown in Fig. 15. They have a peculiar shape, and converge to the diagonal entries of W_{FD}, as expected.

4. *Nonthermal stationary state*

For this example, we start from an (rather arbitrary) initial

$$W(k,0) = \frac{2}{5}\begin{pmatrix} \frac{1}{2}e^{-\cos(4\pi(k-\gamma))} + \frac{1}{4} & \frac{1}{4}\sin(e^{2\pi ik}) \\ \frac{1}{4}\sin(e^{-2\pi ik}) & \frac{1}{4}\mathrm{erf}(\cos(2\pi k)) + \frac{1}{2} + \arctan\left(\sin\left(2\pi k - \frac{1}{5}\right)\right) + \frac{\pi}{4} \end{pmatrix}, \tag{64}$$

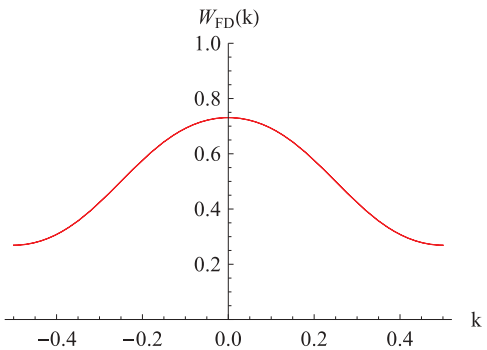

FIG. 12. (Color online) Diagonal matrix entries of an equilibrium state W_{FD} with $\beta = 1$ and same chemical potentials $\mu_\uparrow = \mu_\downarrow = 1$.

illustrated in Fig. 16 (where γ is the Euler gamma constant), and then determine the stationary, nonthermal state $W_{\mathrm{st}}(k)$, via the f function described in Sec. III B. Figure 17 illustrates both f and W_{st}. Next, we run the numerical simulation of the time evolution, which should converge to the predicted $W_{\mathrm{st}}(k)$. Figure 18 indeed verifies the convergence to $W_{\mathrm{st}}(k)$.

For special cases, we have checked that the asymptotic decay rate is almost independent of the initial conditions. This strongly suggests that the collision operator linearized at W_{st} has a spectral gap.

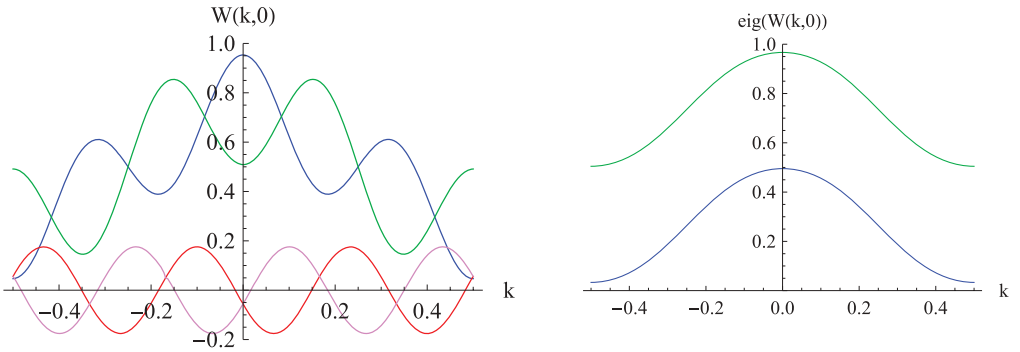

(a) initial $W(k,0)$ (b) eigenvalues of $W(k,0)$

FIG. 13. (Color online) (a) Initial state $W(k,0) = W_{\mathrm{FD}}(k) + V(k)$ with $W_{\mathrm{FD}}(k)$ proportional to the identity matrix (see Fig. 12) and $V(k)$ defined in Eq. (59). The blue (center top) and green (center middle) curves show the real diagonal entries, and the red (lower dark gray) and magenta (lower light gray) curves show the real and imaginary parts of the off-diagonal $|\uparrow\rangle\langle\downarrow|$ entry, respectively. (b) The eigenvalues of $W(k,0)$ are nondegenerate, different from the equilibrium state $W_{\mathrm{FD}}(k)$.

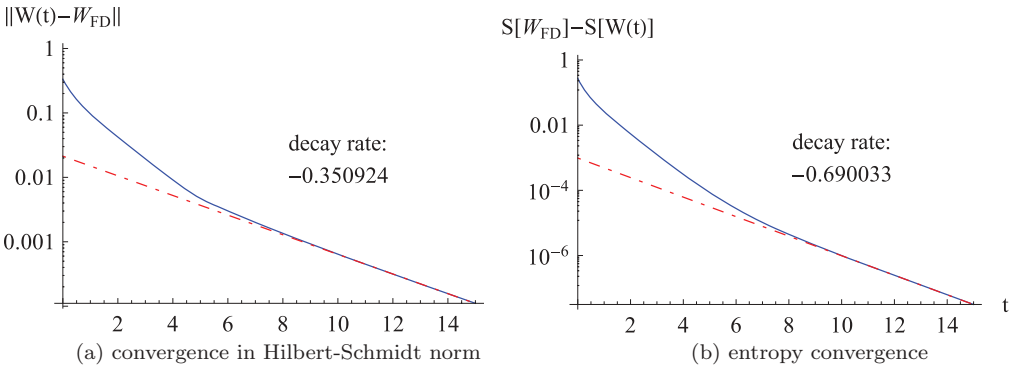

(a) convergence in Hilbert-Schmidt norm (b) entropy convergence

FIG. 14. (Color online) Convergence to the equilibrium state W_{FD} with degenerate eigenvalues (Fig. 12) as a semilogarithmic plot (blue). The decay rate is the slope of the fitted red (dotted) line.

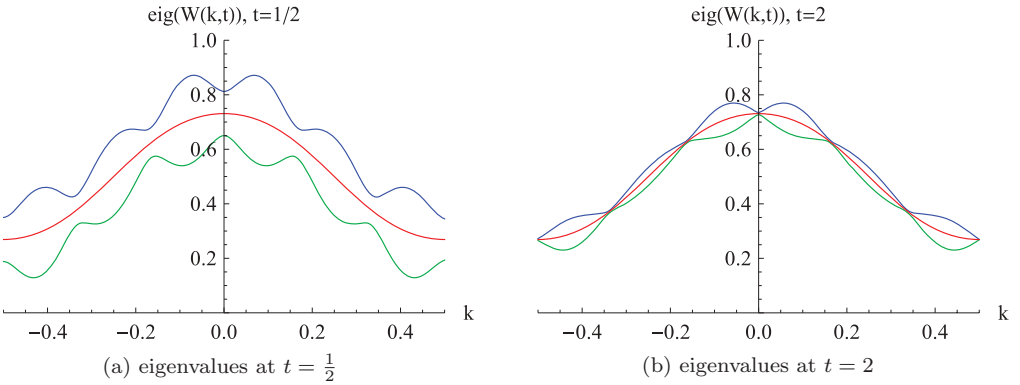

(a) eigenvalues at $t = \frac{1}{2}$ (b) eigenvalues at $t = 2$

FIG. 15. (Color online) Two snapshots showing the convergence of the eigenvalues to the equilibrium state W_{FD} (centered red, same as Fig. 12) with $\mu_\uparrow = \mu_\downarrow = 1$.

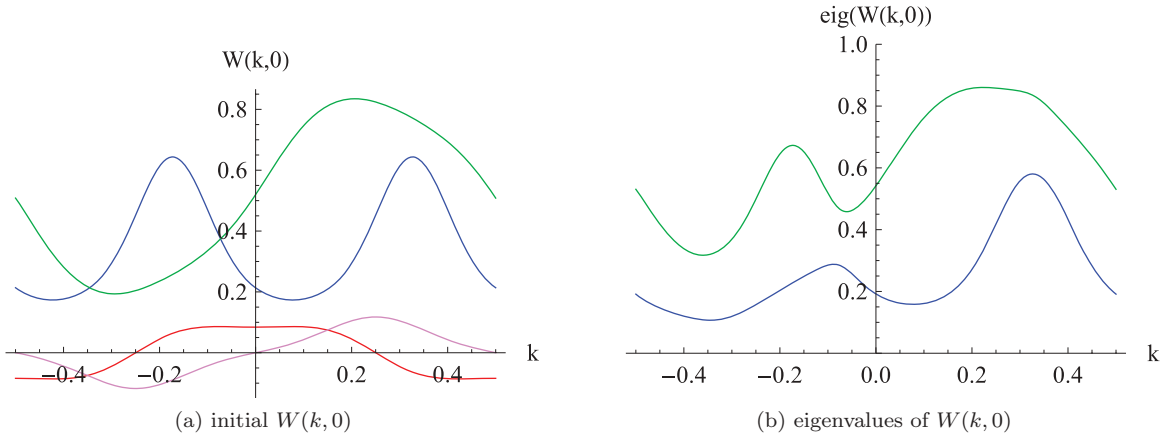

(a) initial $W(k,0)$ (b) eigenvalues of $W(k,0)$

FIG. 16. (Color online) (a) Initial state $W(k,0)$ defined in Eq. (64). The blue (two peaks) and green (upper right) curves show the real diagonal entries, and the red (lower dark gray) and magenta (lower light gray) curves show the real and imaginary parts of the off-diagonal $|\uparrow\rangle\langle\downarrow|$ entry, respectively. (b) Eigenvalues of $W(k,0)$ in the interval $[0,1]$.

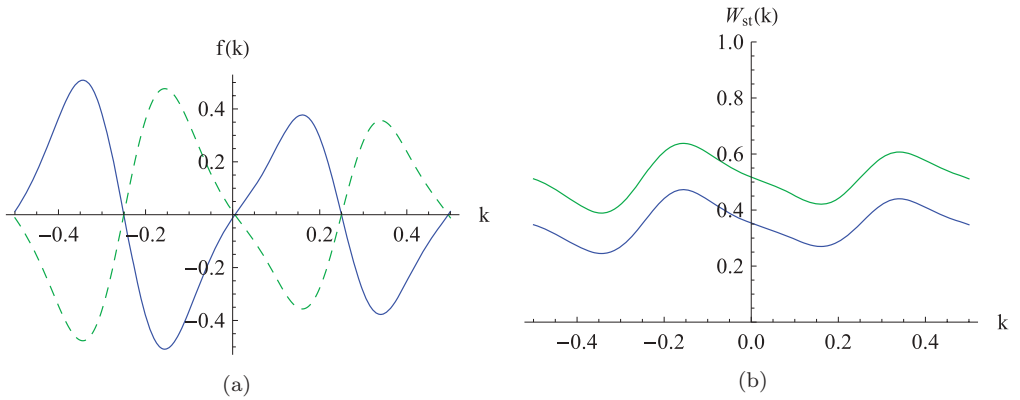

(a) (b)

FIG. 17. (Color online) (a) The f function (solid blue) calculated from $\mathrm{tr}[W(k,0) - W(\frac{1}{2}-k,0)]$ (green dashed) and the fitted "chemical potentials" $a_\uparrow = -0.617485$ and $a_\downarrow = 0.0578622$. The initial $W(k,0)$ is defined in Eq. (64). (b) Resulting stationary state $W_{st}(k)$ [Eq. (39)] given by f and $a_\uparrow, a_\downarrow$.

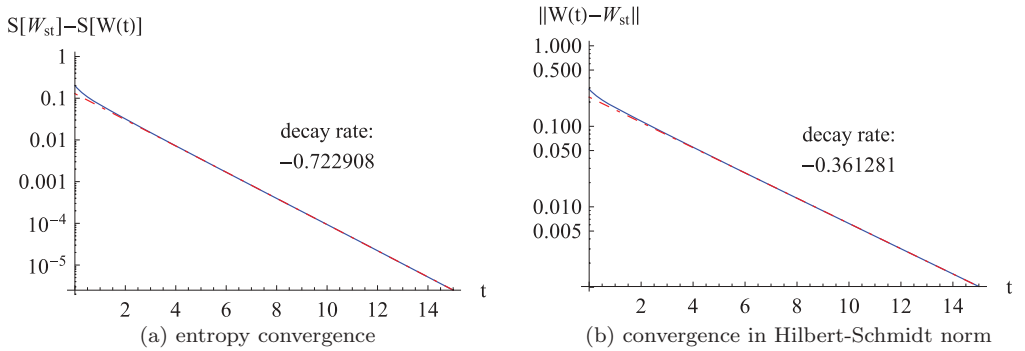

(a) entropy convergence (b) convergence in Hilbert-Schmidt norm

FIG. 18. (Color online) Convergence to the calculated W_{st} (Fig. 17) as a semilogarithmic plot.

VI. CONCLUSIONS

The kinetic equation for the Hubbard model, in general, has two hardly investigated features: (i) the Wigner function is 2×2 matrix valued and (ii) the microscopic SU(2) invariance implies additional conservation laws. We investigated here the chain with nearest-neighbor hopping, which is an integrable model [1]. The Boltzmann transport equation reflects integrability by an infinite number of conserved quantities and non-thermal stationary states. We established the H theorem and classified all stationary states. Adding a next-nearest-neighbor coupling seems to destroy all conservation laws beyond spin and energy, which indicates that now the stationary solutions are exhausted by the thermal Fermi-Dirac Wigner functions.

In the spatially homogeneous case we observed numerically an exponentially fast convergence to the predicted stationary state, both for the diagonal and off-diagonal matrix elements with roughly comparable decay rates. The decay at low temperatures is slower than at high temperatures, as one would have expected. In principle, asymptotic decay rates can be computed from the linearized collision operator.

Physically of great interest would be to better understand the spatially inhomogeneous situation. For example one could imagine to have in each half of the chain a thermal state with the same temperature, but with different spin orientations. In principle, this could be handled by kinetic theory. One only would have to add in the kinetic equation the transport term $\omega'(k)\,\partial/\partial_x$. Numerically, such a problem is more demanding than the one studied here but is, at least in one dimension, still in reach. Another challenging problem would be to study energy transport through the chain. Our results point towards the validity of Fourier's law.

APPENDIX: CHARACTERIZATION OF STATIONARY SOLUTIONS

Proposition 1: Let $\sigma[W]$ be as defined in Eq. (22). If $0 < W < 1$, then the solutions to zero entropy production,

$$\sigma[W] = 0, \tag{A1}$$

are necessarily of the form of Eq. (39).

Remark: As noted by J. Lukkarinen, further zero entropy and stationary solutions are obtained by setting one eigenvalue of W identically $= 0,1$, and the other eigenvalue arbitrary.

Proof: On the one hand, if W is of the form of Eq. (39), then $\sigma[W] = 0$ follows by inserting. On the other hand, let $\sigma[W] = 0$. We set $\boldsymbol{k} = (k_1,k_2,k_3,k_4)$, $\boldsymbol{\sigma} = (\sigma_1,\sigma_2,\sigma_3,\sigma_4)$, $d^4\boldsymbol{k} = dk_1\,dk_2\,dk_3\,dk_4$ and define

$$F(\boldsymbol{k},\boldsymbol{\sigma}) = (\tilde{\varepsilon}_1\tilde{\varepsilon}_2\varepsilon_3\varepsilon_4 - \varepsilon_1\varepsilon_2\tilde{\varepsilon}_3\tilde{\varepsilon}_4)\log\left(\frac{\tilde{\varepsilon}_1\tilde{\varepsilon}_2\varepsilon_3\varepsilon_4}{\varepsilon_1\varepsilon_2\tilde{\varepsilon}_3\tilde{\varepsilon}_4}\right) \geqslant 0, \tag{A2}$$

with the ε_i as in Sec. II; furthermore,

$$G(\boldsymbol{k},\boldsymbol{\sigma}) = |\langle k_1,\sigma_1|k_3,\sigma_3\rangle\langle k_2,\sigma_2|k_4,\sigma_4\rangle - \langle k_1,\sigma_1|k_4,\sigma_4\rangle\langle k_2,\sigma_2|k_3,\sigma_3\rangle|^2. \tag{A3}$$

Then

$$\sigma[W] = \frac{\pi}{4}\int_{\mathbb{T}^4} d^4\boldsymbol{k}\,\delta(\underline{k})\delta(\underline{\omega})\sum_{\boldsymbol{\sigma}} F(\boldsymbol{k},\boldsymbol{\sigma})G(\boldsymbol{k},\boldsymbol{\sigma}), \tag{A4}$$

according to Eq. (26). Since all terms are non-negative,

$$F(\boldsymbol{k},\boldsymbol{\sigma})\,G(\boldsymbol{k},\boldsymbol{\sigma}) = 0 \tag{A5}$$

must hold for all $\boldsymbol{\sigma}$ and all $\boldsymbol{k} \in \gamma_2 \cup \gamma_{\text{diag}}$ (see Fig. 2). On γ_1 one has $F = 0$ and no extra information can be extracted.

F has the structure $(x-y)\log\left(\frac{x}{y}\right)$, which is zero only if $x = y$, equivalently if

$$\log\left(\frac{\tilde{\varepsilon}_1\tilde{\varepsilon}_2\varepsilon_3\varepsilon_4}{\varepsilon_1\varepsilon_2\tilde{\varepsilon}_3\tilde{\varepsilon}_4}\right) = \log\left(\frac{\tilde{\varepsilon}_1}{\varepsilon_1}\right) + \log\left(\frac{\tilde{\varepsilon}_2}{\varepsilon_2}\right) - \log\left(\frac{\tilde{\varepsilon}_3}{\varepsilon_3}\right) - \log\left(\frac{\tilde{\varepsilon}_4}{\varepsilon_4}\right) = 0. \tag{A6}$$

Defining the *collision invariants* as

$$\Phi_\sigma(k) = \log\left(\frac{\tilde{\varepsilon}_\sigma(k)}{\varepsilon_\sigma(k)}\right), \tag{A7}$$

condition (A6) reads

$$\Phi_{\sigma_1}(k_1) + \Phi_{\sigma_2}(k_2) = \Phi_{\sigma_3}(k_3) + \Phi_{\sigma_4}(k_4). \tag{A8}$$

Note that the labeling of eigenvalues $\varepsilon_\uparrow(k)$, $\varepsilon_\downarrow(k)$ and corresponding eigenvectors is arbitrary. Thus without loss of generality we can assume that

$$\langle k_1,\uparrow|\,k_2,\uparrow\rangle \neq 0 \quad \text{and thus} \quad \langle k_1,\downarrow|\,k_2,\downarrow\rangle \neq 0, \tag{A9}$$

for all $k_1,k_2 \in \mathbb{T}$.

Consider the contour γ_2 ($k_1 = k_4$, $k_2 = k_3$) for $\boldsymbol{\sigma} = \uparrow\downarrow\uparrow\downarrow$. In this case, the second term on the right side of Eq. (A3) vanishes, and thus

$$G(\boldsymbol{k},\uparrow\downarrow\uparrow\downarrow) = |\langle k_1,\uparrow|\,k_2,\uparrow\rangle\langle k_1,\downarrow|\,k_2,\downarrow\rangle|^2 > 0, \tag{A10}$$

by construction (A9). Therefore condition (A5) forces $F(\boldsymbol{k},\uparrow\downarrow\uparrow\downarrow) = 0$ on γ_2. Equation (A8) becomes after rearranging terms

$$\Phi_\uparrow(k_1) - \Phi_\downarrow(k_1) = \Phi_\uparrow(k_2) - \Phi_\downarrow(k_2). \tag{A11}$$

Since variables are separated, both sides of Eq. (A11) must be constant, i.e.,

$$\Phi_\uparrow(k) - \Phi_\downarrow(k) = c, \tag{A12}$$

for a fixed $c \in \mathbb{R}$ and all $k \in \mathbb{T}$.

Next, we establish that the basis $|k,\sigma\rangle$ has to be k independent up to a k-dependent phase, which can be chosen such that $|k,\sigma\rangle = |\sigma\rangle$ with $|\uparrow\rangle,|\downarrow\rangle$ a fixed basis in $\mathbb{C}^2$. If $c = 0$ in Eq. (A12), then $\Phi_\uparrow = \Phi_\downarrow$, and it follows that $W(k) = \varepsilon(k)\mathbb{1}$. In particular, one can set $|k,\sigma\rangle = |\sigma\rangle$.

In the other case, $c \neq 0$, consider the contour γ_2 for $\boldsymbol{\sigma} = \uparrow\uparrow\downarrow\downarrow$: $F(\boldsymbol{k},\uparrow\uparrow\downarrow\downarrow)$ is nonzero since

$$\Phi_\uparrow(k_1) + \Phi_\uparrow(k_2) - \Phi_\downarrow(k_2) - \Phi_\downarrow(k_1) = 2c \neq 0, \tag{A13}$$

where we have used Eq. (A12) for the first equality. Thus Eq. (A5) requires that $G(\boldsymbol{k},\uparrow\uparrow\downarrow\downarrow) = 0$ on γ_2. Inserted into the definition Eq. (A3) yields

$$\langle k_1,\uparrow|\,k_2,\downarrow\rangle\langle k_2,\uparrow|k_1,\downarrow\rangle = 0, \tag{A14}$$

for all $k_1,k_2 \in \mathbb{T}$. Since the vectors $|k,\uparrow\rangle$ and $|k,\downarrow\rangle$ are an orthonormal basis of $\mathbb{C}^2$ for each fixed k, Eq. (A14) is equivalent to

$$\langle k_1,\uparrow|\,k_2,\downarrow\rangle = 0, \tag{A15}$$

for all $k_1,k_2 \in \mathbb{T}$. Keeping k_2 fixed, this means that $|k_1,\uparrow\rangle =$ const up to a phase, and similarly $|k_1,\downarrow\rangle =$ const. Without loss of generality the phase factor can be set to 1, leaving invariant the projectors $P_\sigma(k) = |k,\sigma\rangle\langle k,\sigma|$. In summary, $|k,\sigma\rangle = |\sigma\rangle$ and $G(\boldsymbol{k},\boldsymbol{\sigma}) = G(\boldsymbol{\sigma})$.

As final step, consider γ_{diag} for $\boldsymbol{\sigma} = \uparrow\downarrow\uparrow\downarrow$. By direct inspection $G(\uparrow\downarrow\uparrow\downarrow) = 1$, thus Eq. (A5) requires $F(\boldsymbol{k},\uparrow\downarrow\uparrow\downarrow) = 0$. Equation (A8) for $k_2 = \frac{1}{2} - k_1$ and $k_4 = \frac{1}{2} - k_3$ becomes

$$\Phi_\uparrow(k_1) + \Phi_\downarrow\left(\tfrac{1}{2} - k_1\right) = \Phi_\uparrow(k_3) + \Phi_\downarrow\left(\tfrac{1}{2} - k_3\right). \tag{A16}$$

Since variables are separated, both sides must be constant, i.e.,

$$\Phi_\uparrow(k) + \Phi_\downarrow\left(\tfrac{1}{2} - k\right) = \text{const}, \tag{A17}$$

for all $k \in \mathbb{T}$. Combined with Eq. (A12), we obtain

$$\Phi_\sigma(k) + \Phi_\sigma\left(\tfrac{1}{2} - k\right) = \text{const}, \tag{A18}$$

for $\sigma = \uparrow, \downarrow$. One concludes that Φ_σ is necessarily of the form

$$\Phi_\sigma(k) = f_\sigma(k) - a_\sigma \quad \text{with} \quad f_\sigma(k) = -f_\sigma\left(\tfrac{1}{2} - k\right), \tag{A19}$$

for all $k \in \mathbb{T}$ and some $a_\sigma \in \mathbb{R}$. Plugging into Eq. (A12), one deduces that $f_\uparrow(k) - f_\downarrow(k) =$ const and, since $f_\sigma(\frac{1}{4}) = 0$, it follows that $f_\uparrow(k) = f_\downarrow(k) = f(k)$ independent of σ. Summarizing, we arrive at

$$\Phi_\sigma(k) = f(k) - a_\sigma. \tag{A20}$$

Solving Eqs. (A20) and (A7) for $\varepsilon_\sigma(k)$ leads to the claimed form of Eq. (39).

Corollary 2: Under the constraint $0 < W < 1$, all stationary solutions, i.e., all solutions to $\mathcal{C}[W] = 0$, are precisely of the form of Eq. (39):

$$W_{\text{st}}(k) = \sum_{\sigma\in\{\uparrow,\downarrow\}} \lambda_\sigma(k)\,|\sigma\rangle\langle\sigma|, \quad \lambda_\sigma(k) = \left(\mathrm{e}^{f(k)-a_\sigma} + 1\right)^{-1}, \tag{A21}$$

with $f(k) = -f(\frac{1}{2} - k)$ for all $k \in \mathbb{T}$.

Proof: Each W_{st} of the form of Eq. (A21) satisfies $\mathcal{C}[W] = 0$, which can be checked by inserting W_{st} into $\mathcal{C}[W]$: specifically, the commutator Eq. (11) defining $C_{\text{c}}[W_{\text{st}}]$ vanishes since H_{eff} and W_{st} are diagonal. The dissipative collision operator $C_{\text{d}}[W_{\text{st}}]$ is zero due to the symmetry properties of γ_{diag} and the fact that $f(k) = -f(\frac{1}{2} - k)$. On the other hand, let W be a solution of $\mathcal{C}[W] = 0$. Then

$$\frac{\partial}{\partial t} W(k,t) = \mathcal{C}[W](k,t) = 0, \tag{A22}$$

and, in particular,

$$\sigma[W] = \frac{d}{dt} S[W] = 0. \tag{A23}$$

According to Proposition 1, W is of the form of Eq. (A21).

[1] F. Essler, H. Frahm, F. Göhmann, A. Klümper, and V. Korepin, *The One-Dimensional Hubbard Model* (Cambridge University Press, Cambridge, 2005).

[2] H. Fehske, R. Schneider, and A. Weiße, eds., *Computational Many-Particle Physics* (Springer, New York, 2008).

[3] M. Rasetti, *The Hubbard Model: Recent Results* (World Scientific, 1991).

[4] R. Peierls, Ann. Phys. **3**, 1055 (1929).

[5] L. W. Nordheim, Proc. R. Soc. London A **119**, 689 (1928).

[6] E. A. Uehling and G. E. Uhlenbeck, Phys. Rev. **43**, 552 (1933).

[7] U. Schneider, L. Hackermüller, J. P. Ronzheimer, S. Will, S. Braun, T. Best, I. Bloch, E. Demler, S. Mandt, D. Rasch, and A. Rosch, Nature **8**, 213 (2012).

[8] L. Erdős, M. Salmhofer, and H.-T. Yau, J. Stat. Phys. **116**, 367 (2004).

[9] J. Lukkarinen and H. Spohn, J. Stat. Phys. **134**, 1133 (2009).

[10] P. Mei, J. Lukkarinen, and H. Spohn (in preparation).

[11] H. Spohn, J. Stat. Phys. **124**, 1131 (2006).